

A B-integral management strategy in discrete single-crystal fibers: towards direct power scaling of femtosecond sources near 2 μm

Jianlei Wang^{1,3}, Yongguang Zhao¹, Ning Zhang², Wenlong Wei², Chun Wang³, Haohai Yu¹,
Valentin Petrov⁴ and Huaijin Zhang¹

¹ *State Key Laboratory of Crystal Materials and Institute of Crystal Materials, Shandong University, Jinan 250100, China*

² *Jiangsu Key Laboratory of Advanced Laser Materials and Devices, School of Physics and Electronic Engineering, Jiangsu Normal University, Xuzhou 221116, China*

³ *Key Laboratory of Laser & Infrared System, Ministry of Education, Shandong University, Qingdao, 266237, China.*

⁴ *Max Born Institute for Nonlinear Optics and Short Pulse Spectroscopy, Max-Born-Str. 2a, 12489 Berlin, Germany.*

Abstract: We propose a B-integral management strategy for manipulating the nonlinear effects by employing a discrete single-crystal fiber (SCF) configuration, enabling direct amplification of 2- μm femtosecond pulses at high repetition rates without additional pulse picking, stretching and compression. The system delivers an average power of >56 W at 75.45 MHz with extremely high extraction efficiency ($>55\%$) and the near diffraction-limited beam quality ($M^2 < 1.2$). The dynamic evolution of the optical spectra and temporal properties in the power amplifier reveals that detrimental nonlinear effects are largely suppressed due to the low accumulated nonlinear phase shift in the discrete SCF layout.

This peer-reviewed article has been accepted for publication but not yet copyedited or typeset, and so may be subject to change during the production process. The article is considered published and may be cited using its DOI.

This is an Open Access article, distributed under the terms of the Creative Commons Attribution licence (<https://creativecommons.org/licenses/by/4.0/>), which permits unrestricted re-use, distribution, and reproduction in any medium, provided the original work is properly cited.
10.1017/hpl.2025.10032

This straightforward, compact and relatively simple approach is expected to open a new route to the amplification of 2- μm ultrashort pulses at MHz and kHz repetition rates to achieve high average/peak powers, thereby offering exciting prospects for the applications in the modern nonlinear photonics.

Key words: Single crystal fiber, ultrafast amplifier, femtosecond pulses, near diffraction-limited beams, chirp-free amplification

Correspondence to: yongguangzhao@yeah.net; chunwang@sdu.edu.cn; haohaiyu@sdu.edu.cn

1. INTRODUCTION

High-average/peak-power ultrafast lasers in the 2- μm spectral range have attracted considerable interest due to numerous scientific and industrial applications, e.g., laser-driven compact soft X-ray sources through high-order harmonic generation (HHG) with the driving wavelength located at the “sweet spot” for pushing the phase-matched harmonic energy beyond the carbon K-edge [1,2], next-generation laser-driven electron/positron colliders based on the recently proposed Big Aperture Thulium (BAT) laser concept with high true wall-plug efficiency [3], efficient pump sources for generating mid-infrared radiation via frequency down conversion in non-oxide optical crystals that exhibit high nonlinearity but lower bandgap, which prevents pumping at 0.8~1 μm [4], and light sources in particular at high repetition rates for high-accuracy and high signal-to-noise ratio of greenhouse gas detection, and high-precision micromachining of transparent organic materials relying on direct linear absorption of the incident photons [5,6]. The generation of ultrashort pulses in the femtosecond regime primarily relies on mode-locking of lasers in a relatively high-quality-factor cavity, which limits the power scalability due to the inevitable trade-off between the pulse duration and the output average power [7]. Therefore, the amplification of ultrafast lasers in the 2- μm spectral range towards high average/peak power has seen rapid development in the past decade [8-10].

Since the large B-integral, i.e., strong nonlinear phase shift during the amplification process severely limits the power-handling capability, making direct amplification of femtosecond pulses towards high average power difficult [11,12], and it appears to be limited only in the picosecond regime for both conventional bulk and fiber amplifiers operating in the 2- μm spectral range [8,10]. Thus, the chirped-pulse amplification (CPA) [13] system based on pulse stretching and compression is commonly required. To date, femtosecond amplifiers at 2 μm can be categorized

into two main approaches both based on CPA technology, i.e., optical parametric chirped-pulse amplification (OPCPA) in nonlinear crystals [14] and laser CPA in Tm- or Ho-doped gain media [15,16].

Broadband amplification achievable in multi-stage OPCPA systems enables few-cycle pulse generation with multi-mJ pulse energies at kHz repetition rates [17-20], with the resulting multi-tens of GW peak powers capable of high-flux soft X-ray HHG [17]. The downside of such systems is the limited average power due to thermal effects and the relatively low efficiency. In addition, synchronized high-energy picosecond pulses are required from a pump source which inevitably increases complexity and the cost [20,21]. Fiber-based CPA systems are less prone to thermal and thermo-optical effects, making their average power scaling with high beam quality more feasible, but the output energy/peak power is restricted by unwanted nonlinear effects and optical damage [23,24]. Photonic-crystal fibers (PCFs) [25-27] or large-pitch fibers (LPFs) [28-30] can partially overcome these problems and improve the peak power to the GW level [31], but their design and fabrication remain technically challenging. Regarding the nonlinear effects and in particular the self-focusing limitation for further peak-power scaling, coherent beam combining offers a promising new direction for such fiber-based CPA systems [32]. In comparison, energetic pulses (multi-tens of mJ) with high peak power exceeding 10 GW can be achieved employing bulk Tm/Ho crystalline regenerative CPA systems [33,34], but the repetition rate is restricted to few kHz and thermal effects come into play as in the OPCPA systems. Thus, achieving high pulse energies at high repetition rates, i.e., high average powers in the 2- μm spectral range, seems difficult with either of the above-mentioned approaches. In principle, diode-pumped thin-disk and slab geometry amplifiers based on the CPA technique can also be potentially useful for achieving high average power together with high pulse energy as

demonstrated in the 1- μm spectral range [35,36], however, these laser designs are relatively complex to implement near 2- μm [37] which is related to material availability, doping level restrictions and the lower laser gain. As a consequence, such multi-pass geometries require many more passes and greater effort for beam shaping at 2- μm .

In summary, the direct amplification system featured with simplicity and compact structure exhibits a poor power-handling capability of watts level limited by the strong nonlinear phase shift of the femtosecond pulses, and the CPA system is now the preferred method but also remains challenging in the 2- μm spectral range for all the bulk systems (OPCPA), regenerative amplifiers, thin-disk and slab amplifiers due to their inherent technical difficulties.

Herein, we propose a new strategy to significantly reduce the nonlinear phase shift of the laser beam, allowing direct amplification of femtosecond pulses without stretching or compression. It is also capable of operation at the high repetition rate of the seed oscillator without pulse picking, and delivering a record power from the direct femtosecond amplification systems in the 2- μm spectral range. This strategy is implemented in a compact amplifier system employing a discrete Ho:YAG SCFs configuration. The term SCF, which is somewhat misleading but already established, refers to a thin crystal rod typically with a diameter of less than 1 mm and a length of a few centimeters [38], i.e., it designates an intermediate architecture between bulk crystals and optical fibers. In contrast to optical fibers, it is associated with free-space propagation of the laser beam in combination with wave-guiding of the pump light [39-40]. In the 1- μm spectral range, femtosecond pulses have been amplified to an average power as high as 290 W and a peak power exceeding 2 GW in a simple single-stage SCF amplifier, indicating the inherent capability of SCFs for simultaneous handling of high average and peak powers [41,42]. However, materials near 2- μm typically exhibit anomalous dispersion and the narrower gain spectrum, making it

challenging for direct amplification of femtosecond pulses. In this work, by designing a discrete SCF configuration, the accumulated B-integral value can be significantly reduced, thus suppressing the nonlinear effects. As a proof-of-principle study, it shows that a multi-stage SCF amplifier system is capable of straightforward power scaling of 2- μm ultrafast laser sources at high repetition rates with extremely high extraction efficiency and near diffraction-limited beam quality. The spectral and temporal evolution of the femtosecond pulses in the SCF amplifier is investigated in detail, which will be helpful for future designs of such ultrafast SCF amplification systems towards ultrahigh average and peak powers. The strategy employed here confers direct amplification systems with interesting power scaling prospects and may serve as a good reference for conventional bulk and fiber amplifiers.

2. DESIGN AND METHOD

2.1. B-integral management with discrete SCF configuration

To obtain high average power femtosecond pulses at a high repetition rate, it is inevitably accompanied by serious thermal effects in bulk amplifiers, the gain medium doping with a lower concentration of active ions but longer gain region is a straightforward solution. However, the B-integral value (B) will increase in this case due to the continuous accumulation of nonlinear phase shift in the long gain medium (L) [43]:

$$B = \frac{2\pi}{\lambda} \int_0^L n_2(z) I(z) dz \quad (1)$$

where n_0 and n_2 are the linear and nonlinear refraction index, respectively, λ is the wavelength, and I is the beam intensity.

Then, the laser beam starts self-focusing as the peak power exceeds the critical power of $P_{cr} = 3.77\lambda^2/(8\pi n_0 n_2)$ [44], thus leading to a reduction of the achievable gain, degraded beam quality, and even breakup of the amplified pulses. Although the controllable beam waists of the free-space propagation light in the SCF can mitigate nonlinear effects more effectively than that in conventional silica fibers, the laser performance is still adversely affected when amplifying ultrashort pulses at a high-power level, as demonstrated in the Yb-SCF femtosecond laser amplifier [40].

To overcome this limitation, the strategy employed here is based on a discrete layout of the SCFs, which can provide the following advantages: I) prevention of continuous accumulation of nonlinear phase shift, i.e., discrete B-integral values, and II) the length of the SCF is controllable and can be shorter than twice the self-focusing length (Z_f), assuming the average power amplifier reaches P_{max} at the middle of the last-stage SCF amplifier [43]:

$$L < 2Z_f = \frac{2\pi\omega_0^2}{\lambda} \left(\frac{8\pi n_0 n_2 P_{max}}{3\lambda^2} - 1 \right)^{-1/2} \quad (2)$$

where ω_0 is beam waist radius.

This ensures that the laser pulses exit the SCF before beam collapse, analogous to the multiple-plate structure [44], but with a much lower light intensity in our case. With such a discrete configuration of SCFs (three identical SCFs with 50 mm in length, see the next section for more details), the simulated average power can achieve >200 W for 500-fs pulses at a high repetition rate of 50 MHz, with the B-integral value less than π and $2Z_f$ of ~50 mm.

2.2 Experimental setup of the seed source

To perform the direct amplification experiment, **Figure 1** schematically shows the entire SCF amplifier system comprising a femtosecond seed source, pre- and multi-stage SCF amplifiers without temporal pulse stretching or compression. The seed source was a wavelength-tunable

semiconductor saturable absorber mirror (SESAM) mode-locked Tm(2.8 at.%):LuScO₃ ceramic (3×3×3 mm³) laser in-band pumped by a home-made continuous-wave (CW) Er:YAG bulk laser delivering the maximum power of 3.2 W, linearly polarized beam at 1645 nm [45]. The pre-amplifier was a Ho:YAG-SCF pumped by a laser diode (LD) at 1907 nm, and the main amplifier based on three discrete Ho:YAG SCFs was inband pumped by a Tm-fiber laser at 1907 nm.

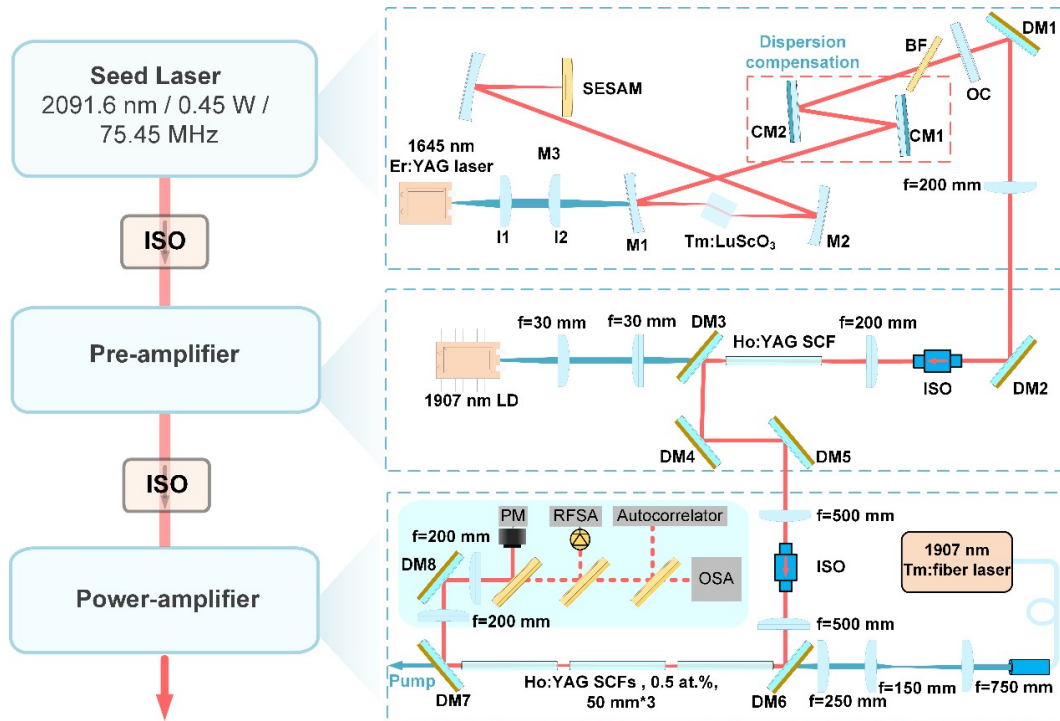


Figure 1. Schematic diagram of the Ho:YAG SCF amplification system. L1/L2: optical collimation/focusing system; M1, M2, M3: concave dichroic mirrors; CM1 and CM2: plane dispersive mirrors; OC: output coupler; BF: birefringent filter; DM: plane dichroic mirror; LD: laser diode.

For the seed laser, as shown in **Figure 1**, the collimated pump beam was focused into the ceramic sample by an aspheric lens (L2, $f = 75$ mm), resulting in a beam diameter of ~ 45 μm . A standard X -shaped astigmatically compensated cavity with a physical length of ~ 2.1 m was employed, in which two plano-concave mirrors, M1 and M2, both with a radius of curvature of $R_{OC} = -100$ mm, formed a beam waist of 30 μm (sagittal) \times 60 μm (tangential) diameter within the Tm:LuScO₃ ceramic placed at Brewster's angle between them. Another plano-concave

mirror (M3) with $R_{OC} = -150$ mm was used to create a second beam waist of 80 μm in diameter on the GaSb-based SESAM [46] for mode-locking. Two chirped mirrors, CM1 and CM2, providing negative group delay dispersion (GDD) of -125 fs^2 and -1000 fs^2 per bounce, respectively, were inserted into the other cavity arm for dispersion compensation. This arm was terminated by the output coupler (OC), a plane-wedged mirror with a transmission of $T_{OC} = 3\%$. A home-made 3-mm-thick quartz birefringent filter (BF), cut with its crystal axis at 24° to the surface normal, was inserted close to the OC at Brewster's angle to tune the wavelength of the femtosecond laser for matching the wavelength of the subsequent SCF amplifiers.

2.3 Experimental setup of the direct femtosecond amplification system

After passing through an optical isolator (ISO), the seed pulse was directly imaged into the pre-amplifier via two lenses ($f = 200$ mm). A 1-mm-diameter (Φ), 50-mm-long $\text{Y}_3\text{Al}_5\text{O}_{12}$ (YAG) SCF doped with 0.3 at.% Ho^{3+} ions served as a pre-amplifier counter-pumped by a 30 W fiber-coupled LD (400- μm core diameter, 0.22 NA) at 1907 nm. The pump light was imaged into the initial part (~ 3 mm from the pump face) of the SCF using a 1:1 telescope system and then waveguided down to the fiber end through total internal reflection. The pre-amplified femtosecond pulses were directly imaged into the power amplifier, where three identical Ho:YAG SCFs ($\Phi 1$ mm \times 50 mm, 0.5 at.% Ho^{3+}) in a serial arrangement with separations of ~ 4 mm were used as gain media. The beam waist with a measured diameter of ~ 460 μm was located in the initial part of the second SCF to ensure free-space propagation of the laser beam in the three-stage-SCF power amplifier. A high beam quality ($M^2 \sim 1.05$) Tm-fiber laser at 1907 nm was employed as a pump source to ensure spatial matching with the beam from the pre-amplifier along the entire SCF power amplifier chain. The pump light was focused into the second SCF to a spot diameter of ~ 450 μm , with a beam size in the three SCFs not exceeding 600 μm in

diameter at any position, thus lengthening the effective gain regions. This makes the experimental setup extremely simple and robust without requiring any re-imaging telescopes. It shall be outlined that all lateral surfaces of the SCFs have been optically polished, and the measured transmission losses were less than 3 dBm^{-1} at 632.8 nm. All input/output SCF faces and all lenses were antireflection-coated. To better mitigate the thermal effects, all the SCFs were mounted in specially designed aluminum modules being in direct contact with cooling water at 13°C .

3. RESULTS AND DISCUSSION

3.1. Seed source and pre-amplifier systems

The output performance of the mode-locked Tm:LuScO₃ laser is shown in **Figure 2**. For a pump power of $\sim 2.5 \text{ W}$, the average output power ranged from 0.24 to 0.35 W when adjusting the intra-cavity BF, corresponding to a tuning spectral span of $\sim 63 \text{ nm}$ ranging from 2044 to 2107 nm, as shown in **Figure 2a**. The autocorrelation traces in **Figure 2b** were recorded by a commercial autocorrelator (APE pulseCheckSM, extended IR), yielding pulse durations (τ) of 195 to 373 fs.

To match the peak wavelength of the Ho:YAG emission spectrum at $\sim 2091 \text{ nm}$, the central wavelength of the seed laser was tuned to 2091.6 nm with a spectral FWHM of $\sim 12 \text{ nm}$, see **Figure 2c**. The average output power at this wavelength reached 0.45 W at a pump power of 3.2 W, corresponding to a single pulse energy of $\sim 6 \text{ nJ}$. The measured autocorrelation trace is presented in **Figure 2d**, and the corresponding pulse duration (FWHM intensity) was 360 fs.

Figures 2e and 2f depict the radio frequency (RF) spectrum of the mode-locked Tm:LuScO₃ seed laser at 2091.6 nm. The fundamental beat note at $\sim 75.45 \text{ MHz}$ exhibited a signal-to-noise ratio (SNR) of $>65 \text{ dBc}$. The uniform harmonic beat notes observed on a 1 GHz span indicate the

absence of spurious modulations and the stable mode-locked operation. The beam quality factor at the maximum average power was $M^2 = 1.01$ and 1.04 in the horizontal (x) and vertical (y) directions, respectively. The inset in **Figure 2d** shows the near-field beam intensity profile, which shows the TEM₀₀ mode of the seed laser. The excellent temporal and spatial features are prerequisites for subsequent amplification in the Ho:YAG SCFs.

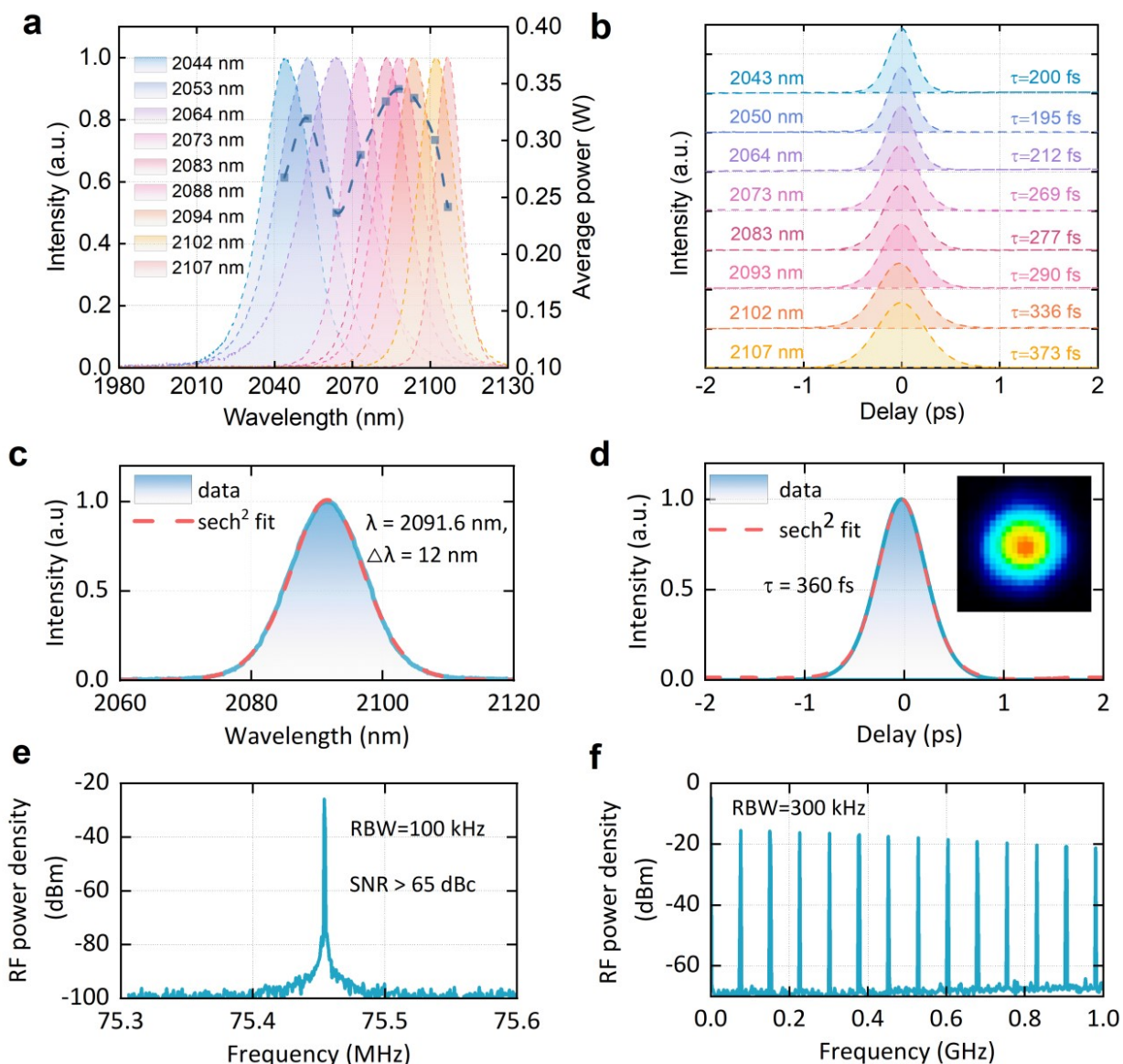


Figure 2. Output performance of the Tm:LuScO₃ laser. **a** Tunable mode-locked operation: spectra and average output power (circles and dashed line), **b** the corresponding autocorrelation traces where τ is the pulse duration (Full Width at Half Maximum, FWHM) assuming sech²-temporal shapes. **c** Optical spectrum, **d** autocorrelation trace with the inset showing the recorded near-field spatial beam profile, **e** radio frequency (RF) spectrum of the fundamental beat note

measured with a resolution bandwidth (RBW) of 100 kHz and **f** RF spectrum on a 1 GHz span (RBW = 300 kHz) at the selected seed wavelength of 2091.6 nm. SNR: signal-to-noise ratio.

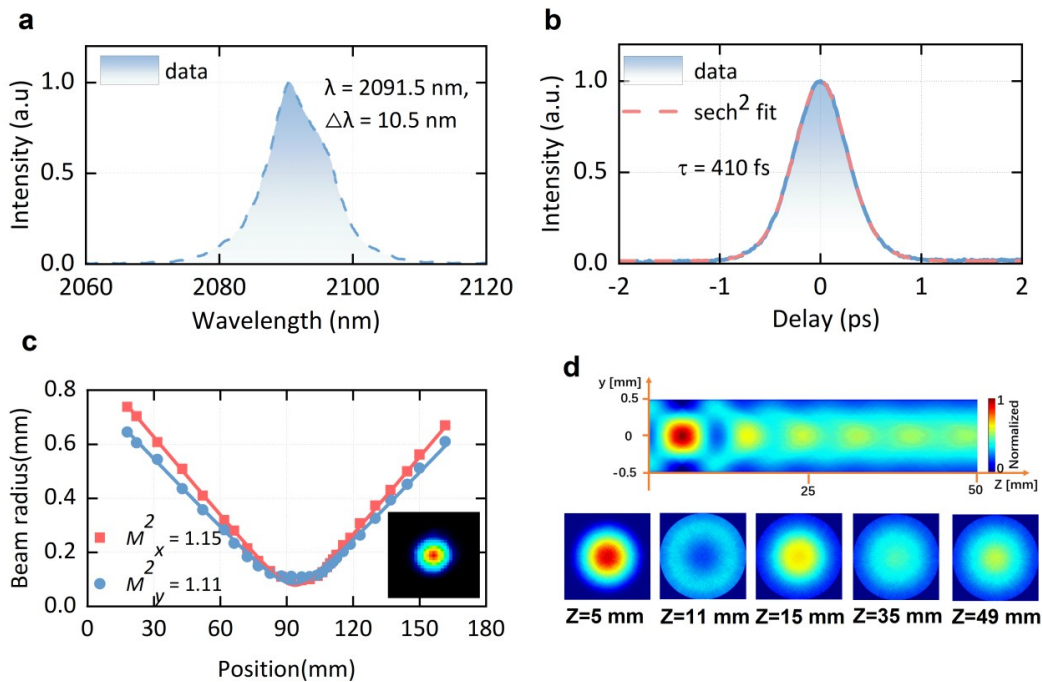


Figure 3. Performance of the Ho:YAG SCF pre-amplifier. **a** Optical spectrum and **b** autocorrelation trace measured after the pre-amplifier. **c** Beam caustics and near-field intensity profile (inset) with fitted M^2 propagation factors. **d** Simulated pump light spatial intensity distribution in the Ho:YAG SCF of the pre-amplifier pumped by the 1907 nm LD with Z indicating the distance from the input pump face.

The Ho:YAG SCF pre-amplifier was designed to increase the average power of the seed laser, and the maximum output power of 0.8 W was reached for an injected seed power of 0.45 W. The amplified pulse spectrum was centered at 2091.5 nm with a FWHM of 10.5 nm, see **Figure 3a**, which corresponded to slightly longer pulses of 410 fs (as shown in **Figure 3b**) attributed to the gain narrowing, as well as slightly affected by material dispersion (see Supplementary Section I for the discussions). The M^2 values measured after the pre-amplifier were only marginally increased, $M_x^2 = 1.11$ and $M_y^2 = 1.15$ in the horizontal and vertical direction, respectively. **Figure 3d** shows the pump intensity distribution in the pre-amplifier under waveguiding conditions, which was simulated by the ray-tracing method. The pump beam was focused into the rear part

of the Ho:YAG SCF with a spot diameter of $\sim 400 \mu\text{m}$, which was well matched to the beam size of the seed laser ranging from ~ 380 to $420 \mu\text{m}$ in the SCF. Following the initial focusing, the pump beam diverged and then was confined through total internal reflection, thus generating multiple pump gain regions along the SCF. The transverse spatial intensity distribution maintained azimuthal uniformity at different locations along the SCF, as shown in **Figure 3d**, which provides favorable conditions for femtosecond pulse amplification compared with traditional rod amplifiers.

3.2. Power scaling in the multi-stage discrete Ho:YAG SCF amplifier concept

The input-output characteristics of the multi-stage Ho:YAG SCF power amplifier were first evaluated by inserting a variable attenuator into the output beam path of the pre-amplifier, enabling continuous adjustment of the injected power without affecting other beam characteristics. The performance of the power amplifier for input average powers P_{in} of 0.1, 0.5, and 0.8 W at a constant pulse duration of ~ 410 fs is shown in **Figure 4**. At $P_{\text{in}} = 0.1$ W, the maximum average output level from the power amplifier reached $P_{\text{out}} = 17.8$ W at ~ 75.45 MHz with an incident pump power of 106 W, corresponding to a slope efficiency of $\eta_{\text{slope}} = 34.2\%$ with respect to the absorbed pump power, and a gain value of ~ 178 . Such a remarkably high gain in the single-pass amplifier is attributed to the high-brightness pumping and the effective mode-matching in the multi-stage SCF configuration. The relatively low output power and slope efficiency at $P_{\text{in}} = 0.1$ W can be attributed to the low extraction capacity at low seed power levels. For $P_{\text{in}} = 0.8$ W and the same incident pump level, P_{out} reached 56.3 W with a slope efficiency of 60.4%, corresponding to a gain value of >70 . Under these conditions, the residual pump power behind the multi-stage SCF power amplifier amounted to only $\sim 5\%$, which leads to an optical extraction efficiency $\eta_{\text{opt}} = (P_{\text{out}} - P_{\text{in}})/P_{\text{abs}}$ of 55.8%. To the best of our knowledge, this is the

highest average power demonstrated from a 2- μm femtosecond solid-state amplifier. The absence of roll-off in the power dependence suggests that further scaling should be possible by increasing the pump power. However, the high gain of the Ho:YAG SCF (particularly at the peak emission wavelength of ~ 2090 nm) induces the generation of self-oscillation when the pump power is further increased, thus limiting the power scaling. This will require optimization of the SCF design, e.g., enhancing signal transmittance of the end facet, tilting the device at a slight angle, or cutting the end face at a small angle, which will disrupt conditions of the self-oscillation and further power scaling is expected. Moreover, the power scaling performance by employing single and double Ho:YAG SCFs as power amplifiers is detailed in Supplementary **Figures S1 and S3**.

Moreover, the self-focusing phenomenon is most likely to occur in the final-stage SCF gain medium theoretically owing to its elevated amplification power (~ 56.3 W), potentially leading to an increased B-integral value. However, based on the self-focusing length (Z_f) and self-focusing critical power (P_{cr}) formulas presented in the main text, even although the pulse peak power is close to the P_{cr} (~ 2.1 MW), the calculated $Z_f \approx 80$ mm substantially exceeds the 50-mm SCF length used experimentally. Consequently, self-focusing phenomenon can be neglected in the discrete SCF configuration, yielding a total B-integral of approximately 0.75. For a 150-mm SCF, Z_f is significantly shorter than the gain medium length, enabling self-focusing process to occur within the crystal. Under this condition, the calculated total B-integral is approximately 8.3, which exceeds the value under the discrete layout condition by almost a factor of 10.

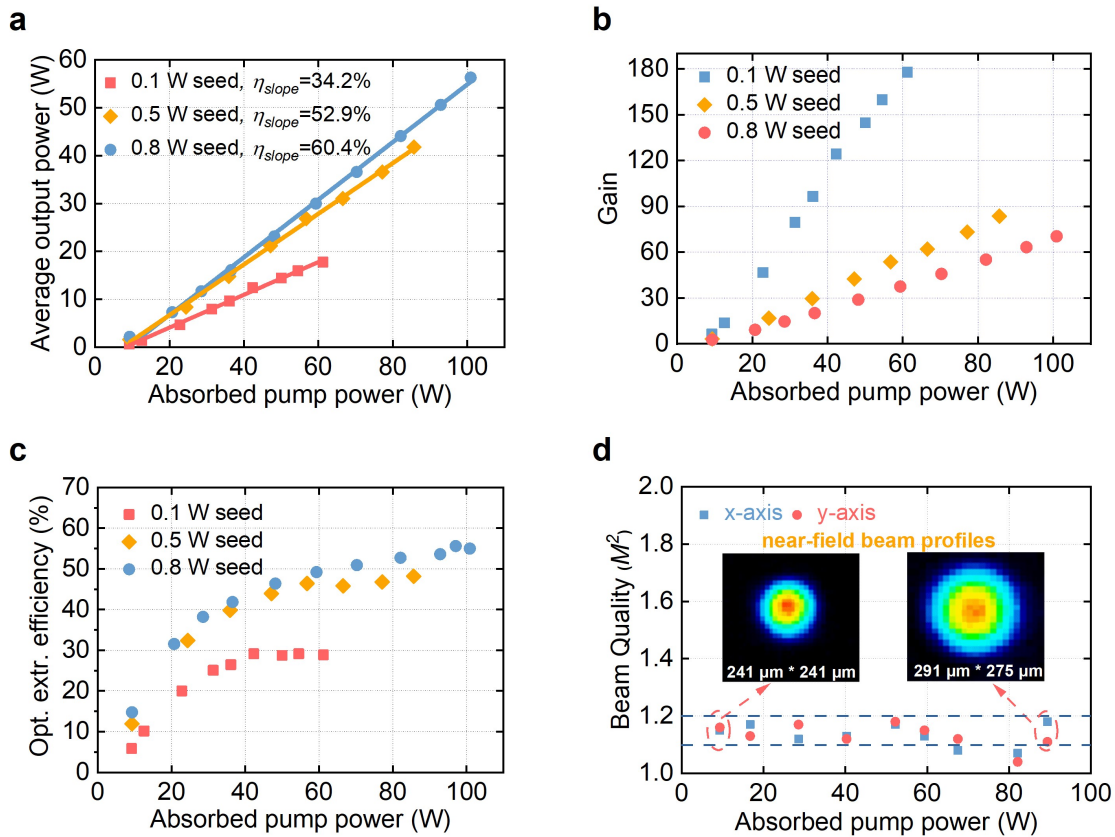


Figure 4. Input-output characteristics of the power amplifier: **a** Measured average output powers, **b** net gain, and **c** optical extraction efficiency versus absorbed pump power for different input levels; η_{slope} : slope efficiency with respect to absorbed pump power. **d** M^2 -factors of the multi-stage Ho:YAG SCF power-amplifier versus absorbed pump power measured at $P_{\text{in}} = 0.8$ W; the insets show near-field output beam profiles recorded at absorbed pump power levels of 10 W (left) and 90 W (right) with x and y designating the horizontal and vertical directions, respectively.

For the maximum $P_{\text{in}} = 0.8$ W, the output beam quality factors at different absorbed pump powers were measured with a Spiricon CCD camera, as shown in **Figure 4d**. The beam quality factors remained below 1.2 over the entire measurement range, which confirms the spatial mode stability of the amplified beam. At an absorbed pump power of ~ 90 W, the beam quality factor was measured to be $M_x^2 = 1.18$ and $M_y^2 = 1.14$ in the horizontal and vertical directions, respectively. It can be concluded that the beam quality of the pre-amplifier is practically maintained in the power amplifier, while thermal stress-induced degradation is suppressed by direct water cooling.

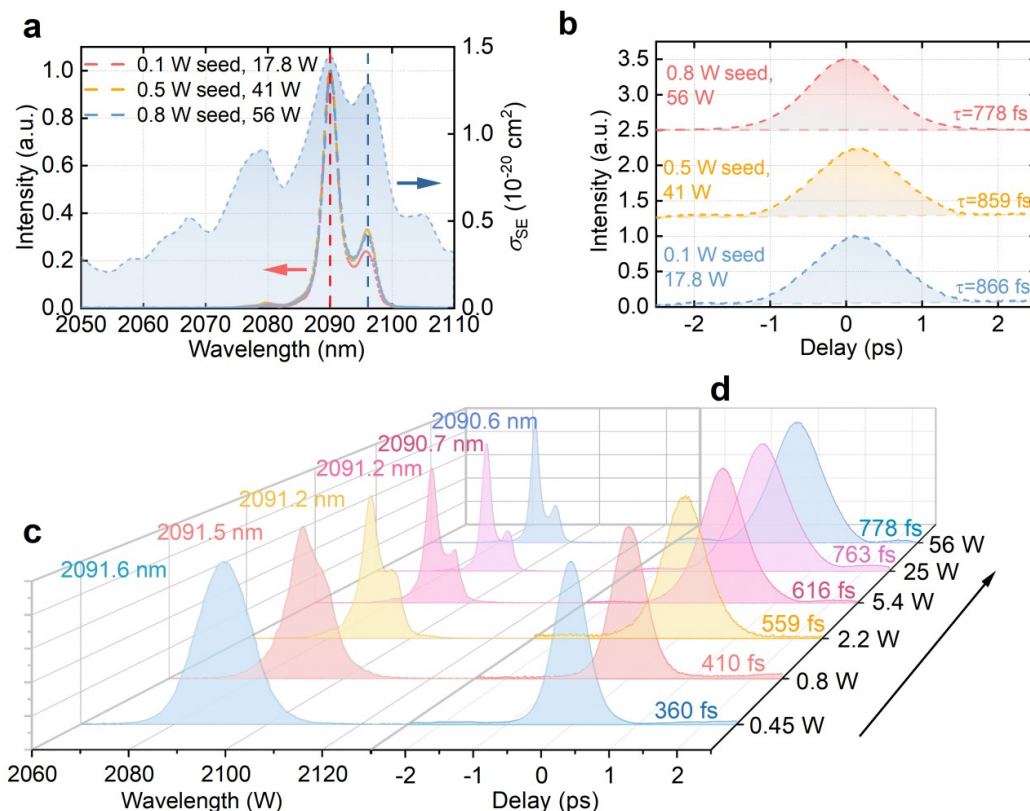


Figure 5. Spectral and temporal performance of the Ho:YAG SCF power amplifier. **a** Spectra and **b** autocorrelation traces measured at the output of the power amplifier chain at the maximum pump level for the three different seed average powers; τ is the derived pulse duration (FWHM intensity). The gray spectrum in **a** and the right scale show the stimulated emission cross section σ_{SE} of Ho:YAG. Dynamic evolution of **c** the optical spectrum and **d** the autocorrelation trace from the seed laser through pre- and power-amplifier at the maximum seed level.

3.3. Dynamic evolution of the optical spectra and temporal properties

The output spectra from the power amplifier under maximum pump power were similar for the three injected power levels of 0.1, 0.5, and 0.8 W, corresponding to pulse durations of 778, 859 and 866 fs, respectively, see **Figures 5a and 5b**. To analyze the spectral and temporal evolution, the measured spectra and pulse durations are summarized in **Figures 5c and 5d** for all stages (including those of the mode-locked laser and the pre-amplifier). Compared with the spectrum of the seed laser centered at ~ 2091.6 nm, the FWHM of the spectra gradually decreased, and the central wavelength shifted to ~ 2090.6 nm. Meanwhile, a weaker spectral peak appeared at ~ 2096

nm, which correlates with the gain spectrum of Ho:YAG (see **Figure 5a**). The spectrum of the power amplifier at the average power of ~ 56 W shows no indication of amplified spontaneous emission (ASE) or nonlinear effects, which highlights the main advantages of the SCF, namely, high overall gain and nonlinear effects suppression. To overcome the gain narrowing in the power-amplifier, an effective solution in future work would be initial spectral shaping with suppressed peak intensity of the seed light [15,47].

The autocorrelation trace at maximum output power of the power-amplifier indicates a pulse duration of 778 fs without any significant pulse distortion. Remarkably, the ultrashort pulse was amplified up to 0.75 μ J pulse energy and 0.84 MW peak power without a stretcher-compressor configuration. Such high performance of the ultrafast amplifier (i.e., high efficiency, high average power and good beam quality) obviously benefited from the long gain region, the nonlinear effects suppression, and large surface-to-volume ratio of the multi-stage Ho:YAG SCF amplification system. Similarly, the dynamic evolution of the optical spectra and temporal properties are shown in Supplementary **Figures S2 and S4**.

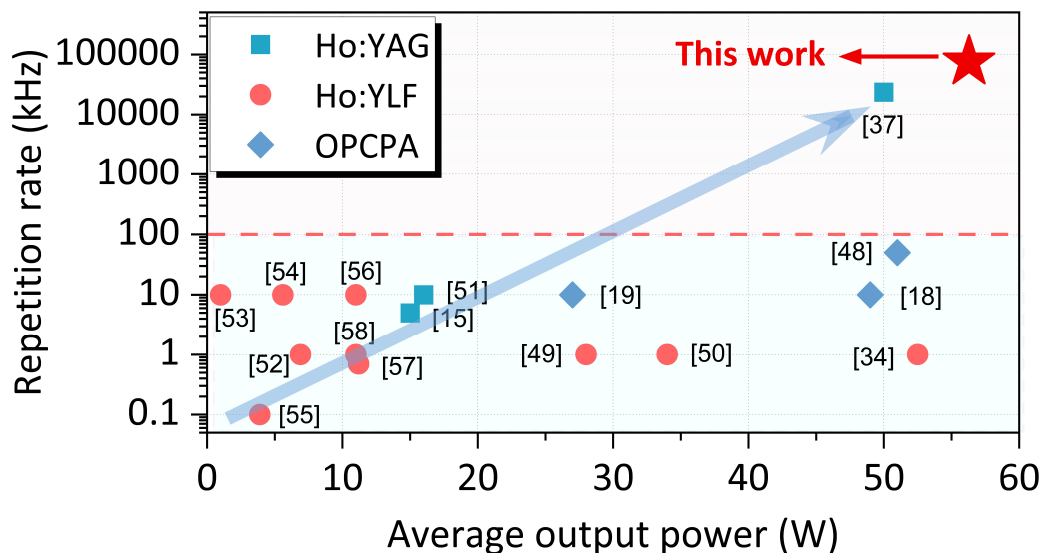


Figure 6. Overview of 2- μ m ultrafast amplifiers based on Ho-doped bulk gain media and OPCPA [15,18,19,34,37,48-58]. Note that, results of direct amplification of femtosecond pulses in conventional fibers are not described here due to their much lower power level.

4. CONCLUSIONS

In conclusion, we have experimentally demonstrated a compact, high-performance multi-stage SCF amplifier for direct amplification of femtosecond pulses at 2 μm without pulse picking, stretching or compression. The multiple SCFs in the power amplifier were designed to lengthen the gain region and provide a uniform heat distribution, which was instrumental in achieving a maximum average power of 56.3 W at 75.45 MHz with a slope efficiency of 60.4% and near-diffraction-limited beam quality ($M^2 < 1.2$). To the best of our knowledge, this laser amplifier has produced the record average power from the direct femtosecond amplification system, and also the highest value among femtosecond solid-state laser and parametric amplifiers in the 2 μm spectral region [15,18,19,34,37,48-58], see **Figure 6**. Simultaneously, it is the only system operating at high repetition rates apart from the long-cavity thin-disk oscillator [37] mode-locked at 23.5 MHz albeit with >1 ps pulse duration. These results show that the developed multi-stage SCF amplifier is an attractive alternative to multi-pass or regenerative amplifiers and at the same time avoids the disadvantages of OPCPA systems (e.g., complexity and price, low efficiency, strict synchronization with pump pulses, etc.).

The novel approach based on multi-stage SCFs is applicable at reduced (kHz) and directly at the high (typically 100 MHz) repetition rate of the femtosecond oscillator and shows potential for further power scaling. Thus, it is promising for applications requiring high average powers with high repetition rates at sub-ps pulse durations, such as laser spectroscopy, high-precision material processing, etc. Further work will focus on optimizing the length and number of the SCFs to further reduce the threshold for nonlinear phase accumulation. This will allow one to extend the present approach to higher single pulse energies at lower repetition rates employing a

pulse picker as well as to shorter pulse durations down to few optical cycles applying post-compression techniques.

Acknowledgement

This work was financially supported by the National Natural Science Foundation of China (62475106, U23A20558, 52025021, 52032009), Natural Science Foundation of Shandong Province, China (ZR2024ZD16), and the Foundation of National Key Laboratory of Plasma Physics (6142A04230301). Y. Zhao acknowledges financial support from the Qilu Young Scholars Program of Shandong University.

Supporting Information

Power scaling performance, dynamic evolution of spectral and temporal properties of direct femtosecond amplification in a single Ho:YAG-SCF amplifier; and in a direct femtosecond amplification system using two discrete SCFs.

References

1. M. Gebhardt, T. Heuermann, R. Klas, C. Liu, A. Kirsche, M. Lenski, Z. Wang, C. Gaida, J. E. Antonio-Lopez, A. Schülzgen, R. Amezcua-Correa, J. Rothhardt, and J. Limpert, “Bright, high-repetition-rate water window soft X-ray source enabled by nonlinear pulse self-compression in an antiresonant hollow-core fibre”, *Light-Sci. Appl.* 10, 36 (2021). DOI: <https://doi.org/10.1038/s41377-021-00477-x>
2. T. Popmintchev, M.-C. Chen, D. Popmintchev, P. Arpin, S. Brown, S. Ališauskas, G. Andriukaitis, T. Balčiunas, O. D. Mücke, A. Pugzlys, A. Baltuška, B. Shim, S. E. Schrauth, A. Gaeta, C. Hernández-García, L. Plaja, A. Becker, A. Jaron-Becker, M. M. Murnane, and H. C. Kapteyn, “Bright Coherent Ultrahigh Harmonics in the keV X-ray

- Regime from Mid-Infrared Femtosecond Lasers”, *Science* 336, 1287-1291 (2012). DOI: <https://doi.org/10.1126/science.1218497>
3. E. Sistrunk, D. A. Alessi, A. Bayramian, K. Chesnut, A. Erlandson, T. C. Galvin, D. Gibson, H. Nguyen, B. Reagan, K. Schaffers, C. W. Siders, T. Spinka, and C. Haefner, “Laser Technology Development for High Peak Power Lasers Achieving Kilowatt Average Power and Beyond”, in *Short-pulse High-energy Lasers and Ultrafast Optical Technologies*, SPIE. (Prague, Czech Republic, 2019), p. 1103407.
 4. V. Petrov, “Frequency down-conversion of solid-state laser sources to the mid-infrared spectral range using non-oxide nonlinear crystals”, *Prog. Quant. Electron.* 42, 1-106 (2015). DOI: <https://doi.org/10.1016/j.pquantelec.2015.04.001>
 5. R. R. Gattass and E. Mazur, “Femtosecond laser micromachining in transparent materials”, *Nat. Photonics* 2, 219-225 (2008). DOI: <https://doi.org/10.1038/nphoton.2008.47>
 6. C. Kerse, H. Kalaycıoğlu, P. Elahi, B. Çetin, D. K. Kesim, Ö. Akçaalan, S. Yavaş, M. D. Aşık, B. Öktem, H. Hoogland, R. Holzwarth, and F. Ö. Ilday, “Ablation-cooled material removal with ultrafast bursts of pulses”, *Nature* 537, 84-88 (2016). DOI: <https://doi.org/10.1038/nature18619>
 7. G. Steinmeyer, D. H. Sutter, L. Gallmann, N. Matuschek, and U. Keller, “Frontiers in Ultrashort Pulse Generation: Pushing the Limits in Linear and Nonlinear Optics”, *Science* 286, 1507-1512 (1999). DOI: <https://doi.org/doi:10.1126/science.286.5444.1507>
 8. M. T. Sohail, B. Li, C. Guo, M. Younis, M. Shareef, M. Abdullah, and P. Yan, “Recent Advancements and Challenges in High-Power Thulium-Doped Laser”, *Adv. Mater. Technol.* 9, 2400496 (2024). DOI: <https://doi.org/10.1002/ADMT.202400496>
 9. D. C. Kirsch, S. Chen, R. Sidharthan, Y. Chen, S. Yoo, and M. Chernysheva, “Short-wave IR ultrafast fiber laser systems: Current challenges and prospective applications”, *J. Appl. Phys.* 128(2020). DOI: <https://doi.org/10.1063/5.0023936>
 10. Z. Chang, L. Fang, V. Fedorov, C. Geiger, S. Ghimire, C. Heide, N. Ishii, J. Itatani, C. Joshi, Y. Kobayashi, P. Kumar, A. Marra, S. Mirov, I. Petrushina, M. Polyanskiy, D. A. Reis, S. Tochitsky, S. Vasilyev, L. Wang, Y. Wu, and F. Zhou, “Intense infrared lasers for strong-field science”, *Adv. Opt. Photon.* 14, 652-782 (2022). DOI: <https://doi.org/10.1364/AOP.454797>

11. Z. Li, Y. Leng, and R. Li, “Further Development of the Short-Pulse Petawatt Laser: Trends, Technologies, and Bottlenecks”, *Laser Photonics Rev.* 17, 2100705 (2023). DOI: <https://doi.org/10.1002/lpor.202100705>
12. J. Rothhardt, S. Hädrich, J. Delagnes, E. Cormier, and J. Limpert, “High Average Power Near-Infrared Few-Cycle Lasers”, *Laser Photonics Rev.* 11, 1700043 (2017). DOI: <https://doi.org/10.1002/lpor.201700043>
13. D. Strickland and G. Mourou, “Compression of amplified chirped optical pulses”, *Opt. Commun.* 55, 447-449 (1985). DOI: [https://doi.org/10.1016/0030-4018\(85\)90151-8](https://doi.org/10.1016/0030-4018(85)90151-8)
14. J. Pupeikis, P. A. Chevreuil, N. Bigler, L. Gallmann, C. R. Phillips, and U. Keller, “Water window soft x-ray source enabled by a 25 W few-cycle 2.2 μm OPCPA at 100 kHz”, *Optica* 7, 168-171 (2020). DOI: <https://doi.org/10.1364/OPTICA.379846>
15. P. Malevich, G. Andriukaitis, T. Flöry, A. J. Verhoef, A. Fernández, S. Ališauskas, A. Pugžlys, A. Baltuška, L. H. Tan, C. F. Chua, and P. B. Phua, “High energy and average power femtosecond laser for driving mid-infrared optical parametric amplifiers”, *Opt. Lett.* 38, 2746-2749 (2013). DOI: <https://doi.org/10.1364/OL.38.002746>
16. Z. Wang, T. Heuermann, M. Gebhardt, M. Lenski, P. Gierschke, R. Klas, J. Rothhardt, C. Jauregui, and J. Limpert, “Nonlinear pulse compression to sub-two-cycle, 1.3 mJ pulses at 1.9 μm wavelength with 132 W average power”, *Opt. Lett.* 48, 2647-2650 (2023). DOI: <https://doi.org/10.1364/OL.487587>
17. K.-H. Hong, C.-J. Lai, J. P. Siqueira, P. Krogen, J. Moses, C.-L. Chang, G. J. Stein, L. E. Zapata, and F. X. Kärtner, “Multi-mJ, kHz, 2.1 μm optical parametric chirped-pulse amplifier and high-flux soft x-ray high-harmonic generation”, *Opt. Lett.* 39, 3145-3148 (2014). DOI: <https://doi.org/10.1364/OL.39.003145>
18. M. F. Seeger, D. Kammerer, J. Blöchl, M. Neuhaus, V. Pervak, T. Nubbemeyer, and M. F. Kling, “49 W carrier-envelope-phase-stable few-cycle 2.1 μm OPCPA at 10 kHz”, *Opt. Express* 31, 24821-24834 (2023). DOI: <https://doi.org/10.1364/OE.493326>
19. T. Feng, A. Heilmann, M. Bock, L. Ehrentraut, T. Witting, H. Yu, H. Stiel, S. Eisebitt, and M. Schnürer, “27 W 2.1 μm OPCPA system for coherent soft X-ray generation operating at 10 kHz”, *Opt. Express* 28, 8724-8733 (2020). DOI: <https://doi.org/10.1364/OE.386588>

20. L. von Grafenstein, M. Bock, D. Ueberschaer, E. Escoto, A. Koç, K. Zawilski, P. Schunemann, U. Griebner, and T. Elsaesser, “Multi-millijoule, few-cycle 5 μm OPCPA at 1 kHz repetition rate”, *Opt. Lett.* 45, 5998-6001 (2020). DOI: <https://doi.org/10.1364/OL.402562>
21. M. Galletti, P. Oliveira, M. Galimberti, M. Ahmad, G. Archipovaite, N. Booth, E. Dilworth, A. Frackiewicz, T. Winstone, I. Musgrave, and C. Hernandez-Gomez, “Ultra-broadband all-OPCPA petawatt facility fully based on LBO”, *High Power Laser Sci. Eng.* 8, e31 (2020). DOI: <https://doi.org/10.1017/hpl.2020.31>
22. S. Klingebiel, C. Wandt, C. Skrobol, I. Ahmad, S. A. Trushin, Z. Major, F. Krausz, and S. Karsch, “High energy picosecond Yb:YAG CPA system at 10 Hz repetition rate for pumping optical parametric amplifiers”, *Opt. Express* 19, 5357-5363 (2011). DOI: <https://doi.org/10.1364/OE.19.005357>
23. D. J. Richardson, J. Nilsson, and W. A. Clarkson, “High power fiber lasers: current status and future perspectives”, *J. Opt. Soc. Am. B* 27, B63-B92 (2010). DOI: <https://doi.org/10.1364/JOSAB.27.000B63>
24. J. Zuo and X. Lin, “High-Power Laser Systems”, *Laser Photonics Rev.* 16, 2100741 (2022). DOI: <https://doi.org/10.1002/lpor.202100741>
25. J. C. Knight, “Photonic crystal fibres”, *Nature* 424, 847-851 (2003). DOI: <https://doi.org/10.1038/nature01940>
26. J. M. Dudley and J. R. Taylor, “Ten years of nonlinear optics in photonic crystal fibre”, *Nat. Photonics* 3, 85-90 (2009). DOI: <https://doi.org/10.1038/nphoton.2008.285>
27. C. Gaida, M. Gebhardt, T. Heuermann, F. Stutzki, C. Jauregui, and J. Limpert, “Ultrafast thulium fiber laser system emitting more than 1 kW of average power”, *Opt. Lett.* 43, 5853-5856 (2018). DOI: <https://doi.org/10.1364/OL.43.005853>
28. F. Stutzki, C. Gaida, M. Gebhardt, F. Jansen, C. Jauregui, J. Limpert, and A. Tünnermann, “Tm-based fiber-laser system with more than 200 MW peak power”, *Opt. Lett.* 40, 9-12 (2015). DOI: <https://doi.org/10.1364/OL.40.000009>
29. M. Baumgartl, F. Jansen, F. Stutzki, C. Jauregui, B. Ortaç, J. Limpert, and A. Tünnermann, “High average and peak power femtosecond large-pitch photonic-crystal-fiber laser”, *Opt. Lett.* 36, 244-246 (2011). DOI: <https://doi.org/10.1364/OL.36.000244>

30. S. Février, B. Beaudou, and P. Viale, “Understanding origin of loss in large pitch hollow-core photonic crystal fibers and their design simplification”, *Opt. Express* 18, 5142-5150 (2010). DOI: <https://doi.org/10.1364/OE.18.005142>
31. C. Gaida, M. Gebhardt, F. Stutzki, C. Jauregui, J. Limpert, and A. Tünnermann, “Thulium-doped fiber chirped-pulse amplification system with 2 GW of peak power”, *Opt. Lett.* 41, 4130-4133 (2016). DOI: <https://doi.org/10.1364/OL.41.004130>
32. T. Heuermann, Z. Wang, M. Lenski, M. Gebhardt, C. Gaida, M. Abdelaal, J. Buldt, M. Müller, A. Klenke, and J. Limpert, “Ultrafast Tm-doped fiber laser system delivering 1.65-mJ, sub-100-fs pulses at a 100-kHz repetition rate”, *Opt. Lett.* 47, 3095-3098 (2022). DOI: <https://doi.org/10.1364/OL.459385>
33. L. von Grafenstein, M. Bock, D. Ueberschaer, U. Griebner, and T. Elsaesser, “Ho:YLF chirped pulse amplification at kilohertz repetition rates 4.3 ps pulses at 2 μm with GW peak power”, *Opt. Lett.* 41, 4668-4671 (2016). DOI: <https://doi.org/10.1364/OL.41.004668>
34. L. von Grafenstein, M. Bock, D. Ueberschaer, A. Koç, U. Griebner, and T. Elsaesser, “2.05 μm chirped pulse amplification system at a 1 kHz repetition rate – 2.4 ps pulses with 17 GW peak power”, *Opt. Lett.* 45, 3836-3839 (2020). DOI: <https://doi.org/10.1364/OL.395496>
35. J. Drs, J. Fischer, N. Modsching, F. Labaye, M. Müller, V. J. Wittwer, and T. Südmeyer, “A Decade of Sub-100-fs Thin-Disk Laser Oscillators”, *Laser Photonics Rev.* 17, 2200258 (2023). DOI: <https://doi.org/10.1002/lpor.202200258>
36. S. Goncharov, K. Fritsch, and O. Pronin, “110 MW thin-disk oscillator”, *Opt. Express* 31, 25970-25977 (2023). DOI: <https://doi.org/10.1364/OE.491938>
37. S. Tomilov, Y. Wang, M. Hoffmann, J. Heidrich, M. Golling, U. Keller, and C. J. Saraceno, “50-W average power Ho:YAG SESAM-modelocked thin-disk oscillator at 2.1 μm ”, *Opt. Express* 30, 27662-27673 (2022). DOI: <https://doi.org/10.1364/OE.460298>
38. X. Délen, A. Aubourg, L. Deyra, F. Lesparre, I. Martial, J. Didierjean, F. Balembois, and P. Georges, “Single crystal fiber for laser sources”, in *Solid State Lasers XXIV: Technology and Devices*, SPIE. (San Francisco, CA, USA, 2015), p. 934202.

39. J. Liu, J. Dong, Y. Wang, J. Guo, Y. Xue, J. Xu, Y. Zhao, X. Xu, H. Yu, Z. Wang, X. Xu, W. Chen, and V. Petrov, “Tm:YAG single-crystal fiber laser”, *Opt. Lett.* 46, 4454-4457 (2021). DOI: <https://doi.org/10.1364/OL.434618>
40. Y. Zhao, C. Zheng, Z. Huang, Q. Gao, J. Dong, K. Tian, Z. Yang, W. Chen, and V. Petrov, “Twisted Light in a Single-Crystal Fiber: Toward Undistorted Femtosecond Vortex Amplification”, *Laser Photonics Rev.* 16, 2200503 (2022). DOI: <https://doi.org/10.1002/lpor.202200503>
41. F. Beirow, M. Eckerle, T. Graf, and M. A. Ahmed, “Amplification of radially polarized ultra-short pulsed radiation to average output powers exceeding 250 W in a compact single-stage Yb:YAG single-crystal fiber amplifier”, *Appl. Phys. B* 126, 148 (2020). DOI: <https://doi.org/10.1007/s00340-020-07502-8>
42. X. Délen, Y. Zaouter, I. Martial, N. Aubry, J. Didierjean, C. Hönninger, E. Mottay, F. Balembois, and P. Georges, “Yb:YAG single crystal fiber power amplifier for femtosecond sources”, *Opt. Lett.* 38, 109-111 (2013). DOI: <https://doi.org/10.1364/OL.38.000109>
43. W. Koechner, *Solid-state Laser Engineering*. (Springer Berlin Heidelberg, 2013), p. 202.
44. C.-H. Lu, Y.-J. Tsou, H.-Y. Chen, B.-H. Chen, Y.-C. Cheng, S.-D. Yang, M.-C. Chen, C.-C. Hsu, and A. H. Kung, “Generation of intense supercontinuum in condensed media”, *Optica* 1, 400-406 (2014). DOI: <https://doi.org/10.1364/OPTICA.1.000400>
45. N. Zhang, P. Wang, B. Chen, Z. Wang, S. Liu, Y. Zhao, Z. Jia, B. Zhang, and Z. Sun, “High-efficiency broadband (> 210 nm) in-band pumped Tm:LuGGG solid-state laser”, *Appl. Phys. B* 128, 128 (2022). DOI: <https://doi.org/10.1007/s00340-022-07852-5>
46. N. Zhang, Q. Song, J. Zhou, J. Liu, S. Liu, H. Zhang, X. Xu, Y. Xue, J. Xu, W. Chen, Y. Zhao, U. Griebner, and V. Petrov, “44-fs pulse generation at 2.05 μm from a SESAM mode-locked Tm:GdScO₃ laser”, *Opt. Lett.* 48, 510-513 (2023). DOI: <https://doi.org/10.1364/OL.480400>
47. P. Malevich, T. Kanai, H. Hoogland, R. Holzwarth, A. Baltuška, and A. Pugžlys, “Broadband mid-infrared pulses from potassium titanyl arsenate/zinc germanium phosphate optical parametric amplifier pumped by Tm, Ho-fiber-seeded Ho:YAG chirped-pulse amplifier”, *Opt. Lett.* 41, 930-933 (2016). DOI: <https://doi.org/10.1364/OL.41.000930>

48. P. Gierschke, C. Grebing, M. Abdelaal, M. Lenski, J. Buldt, Z. Wang, T. Heuermann, M. Mueller, M. Gebhardt, J. Rothhardt, and J. Limpert, “Nonlinear pulse compression to 51-W average power GW-class 35-fs pulses at 2- μm wavelength in a gas-filled multi-pass cell”, *Opt. Lett.* 47, 3511-3514 (2022). DOI: <https://doi.org/10.1364/OL.462647>
49. K. Murari, F. Zhou, Y. Yin, Y. Wu, B. Weaver, T. Avni, E. Larsen, and Z. Chang, “Ho:YLF amplifier with Ti:Sapphire frontend for pumping mid-infrared optical parametric amplifier”, *Appl. Phys. Lett.* 117, 141102(2020). DOI: <https://doi.org/10.1063/5.0021438>
50. L. von Grafenstein, M. Bock, D. Ueberschaer, U. Griebner, and T. Elsaesser, “Picosecond 34 mJ pulses at kHz repetition rates from a Ho:YLF amplifier at 2 μm wavelength”, *Opt. Express* 23, 33142-33149 (2015). DOI: <https://doi.org/10.1364/OE.23.033142>
51. I. Astrauskas, B. Považay, A. Baltuška, and A. Pugžlys, “Influence of 2.09- μm pulse duration on through-silicon laser ablation of thin metal coatings”, *Opt. Laser Technol.* 133, 106535 (2021). DOI: <https://doi.org/10.1016/j.optlastec.2020.106535>
52. P. Kroetz, A. Ruehl, G. Chatterjee, A.-L. Calendron, K. Murari, H. Cankaya, P. Li, F. X. Kärtner, I. Hartl, and R. J. Dwayne Miller, “Overcoming bifurcation instability in high-repetition-rate Ho:YLF regenerative amplifiers”, *Opt. Lett.* 40, 5427-5430 (2015). DOI: <https://doi.org/10.1364/OL.40.005427>
53. M Hinkelmann, D Wandt, U Morgner, J Neumann, and D Kracht, “Ultrashort pulse CPA-free Ho:YLF linear amplifier”, in *Solid State Lasers XXVII: Technology and Devices*, SPIE. (San Francisco, CA, USA, 2018), p. 22-27.
54. M. Hinkelmann, D. Wandt, U. Morgner, J. Neumann, and D. Kracht, “High repetition rate, μJ -level, CPA-free ultrashort pulse multipass amplifier based on Ho:YLF”, *Opt. Express* 26, 18125-18130 (2018). DOI: <https://doi.org/10.1364/OE.26.018125>
55. M. Hemmer, D. Sánchez, M. Jelínek, V. Smirnov, H. Jelinkova, V. Kubeček, and J. Biegert, “2- μm wavelength, high-energy Ho:YLF chirped-pulse amplifier for mid-infrared OPCPA”, *Opt. Lett.* 40, 451-454 (2015). DOI: <https://doi.org/10.1364/OL.40.000451>

56. L. von Grafenstein, M. Bock, U. Griebner, and T. Elsaesser, “High-energy multi-kilohertz Ho-doped regenerative amplifiers around 2 μm ”, *Opt. Express* 23, 14744-14752 (2015). DOI: <https://doi.org/10.1364/OE.23.014744>
57. L. von Grafenstein, M. Bock, G. Steinmeyer, U. Griebner, and T. Elsaesser, “Taming chaos: 16 mJ picosecond Ho:YLF regenerative amplifier with 0.7 kHz repetition rate”, *Laser Photonics Rev.* 10, 123-130 (2016). DOI: <https://doi.org/10.1002/lpor.201500213>
58. D. Alex, “High-energy, kHz-rate, picosecond, 2- μm laser pump source for mid-IR nonlinear optical devices”, in *Solid State Lasers XXII: Technology and Devices*, SPIE. (San Francisco, CA, USA, 2013), p. 46-59.